

JOURNAL of CIVIL ENGINEERING and MANAGEMENT

2025 Volume 31 Issue 7 Pages 783–801

https://doi.org/10.3846/jcem.2025.24607

EVALUATION MODEL OF CONSTRUCTION QUALITY DATA UNCERTAINTY: A STUDY BASED ON INDUSTRY PARK PROJECT

Changhao FU¹, Weijie XU^{1⊠}, Junchi LIU¹, Qingzi GE², Hang BAI², Tong GUO², Tao WANG³

- ¹School of Civil Engineering, Southeast University, Nanjing 211189, China
- ²Sichuan Institute of Building Research, Chengdu 610081, China
- ³China Railway Jinan Group Co., Ltd., Jinan 250102, China

Article History:

- received 13 January 2025
- accepted 30 April 2025

Abstract. This study proposes an evaluation and adjustment model for construction quality data uncertainty based on the research project of the Sichuan Provincial Building Industry Park. The core objective is to address the variability in concrete strength data caused by multiple factors during the construction process through a data-driven approach, which enables the accurate prediction of concrete strength. By analyzing construction quality data across different strength grades and curing ages, this study establishes a dynamic model centered on "data fitting" and "data prediction". The model defines a reliability range for construction quality specific to the project, which facilitates the cleansing of outlier data and the adjustment of biased data. The results demonstrate that the model significantly enhances the reliability of the construction quality data. Further analysis of data from the same construction site revealed that it is highly applicable, and the date adjustment become more concentrated and stable. The fitting coefficient of this model approaches 1, which significantly improving the representativeness and reliability of the strength data. The findings provide a scientific basis for the dynamic assessment and optimization of construction quality, and robust support for quality control and prediction during the construction process.

Keywords: construction quality management, uncertainty evaluation, strength prediction, data adjustment model, dynamic assessment.

1. Introduction

Concrete is the most widely used construction material in the world (Wang et al., 2024a) due to its durability, costeffectiveness, and versatility (Arora et al., 2019; Ren et al., 2019; Cao et al., 2019; Graybeal, 2007). Among the various performance indicators of concrete, compressive strength is one of the most fundamental metrics (Kaboosi et al., 2020; Poorarbabi et al., 2020). It is directly related to the safety and quality of construction projects and serves as a critical parameter for the lifecycle assessment of buildings (Asteris et al., 2021a). Concrete is composed of various components, including cementitious materials, aggregates, and admixtures (Yang et al., 2012). These components are randomly distributed within the concrete matrix, which results in varying strength grades. In many construction sites worldwide, concrete strength and construction quality deeply depend on mix designs informed by past experience. Furthermore, compressive strength testing of concrete is typically performed by construction personnel, and this process can be influenced by subjective judgments and operational methods. Environmental variations also exacerbate potential errors. Such complexities present significant challenges to the accuracy of concrete compressive strength measurements (Feng & Li, 2016; Feng et al., 2016).

The most direct method for obtaining concrete strength is through physical testing, which is both accurate and reliable (Zhou & Zhang, 2011). However, this approach has certain limitations, such as the need to prepare a large number of cubic or cylindrical specimens and its inability to cover all curing ages. Concrete strength data exhibit significant uncertainty, posing multidimensional risks to construction projects. Studies have shown that systematic bias in strength assessment can markedly reduce the safety margin of structures under extreme loading conditions (Akalin et al., 2010). From a quality-control perspective, construction disputes involving concrete are often attributed to inadequate management of measurement uncertainty, particularly when early-age strength test results

[™]Corresponding author. E-mail: xuweijie@seu.edu.cn

exceed the dispersion limits recommended by international standards (Yudhistira et al., 2024). Field evidence further confirms a significant positive correlation between fluctuations in strength data and life-cycle maintenance costs of structures (Soilan et al., 2022). Moreover, the fixed-tolerance approach adopted in current standards has been repeatedly criticized for its high risk of misjudgment (Chen et al., 2023). Consequently, empirical regression methods are often introduced to predict the compressive strength of concrete at various curing ages based on compressive strength tests. Nevertheless, concrete strength exhibits significant variability and strong nonlinearity (Zain & Abd, 2009; Bharatkumar et al., 2001), which make it challenging to derive precise regression expressions. Additionally, numerical simulation serves as another means of estimating concrete strength (Wang et al., 2024b). However, similar to the issues mentioned earlier, the randomness and nonlinear characteristics of strength make it difficult for this method to deliver optimal predictive results.

The causes of uncertainty in concrete strength can be attributed to three main factors: (1) uncertainty arising from nonlinearity; (2) the complexity of causal relationships, which are challenging to express using modern mathematical constitutive relations; and (3) scientific problems with unclear causality. In recent years, with the rapid development of artificial intelligence technologies, machine learning-based predictions of concrete compressive strength have become a growing trend (Najafabadi et al., 2015) and have been widely applied in civil engineering. As shown in Table 1, machine learning algorithms, particularly Support Vector Machines (SVM), Genetic Algorithms (GA), and Artificial Neural Networks (ANN), can capture complex nonlinear relationships from large datasets, which enable more accurate predictions. For example, some scholars (Erdal et al., 2018) predicted the compressive strength of vacuum-treated concrete using artificial neural networks and multivariate regression techniques. Meanwhile, they compared the performance of single and multivariate regression models. One other research (Lorenzi et al., 2017) demonstrated that ANN-based predictions could achieve accurate compressive strength estimates at relatively low computational costs. There is a study (Li et al., 2024) that proposed an SVM-based model for predicting concrete compressive strength, which achieved satisfactory results by considering multiple factors such as material composition and construction processes. Similarly, other scholars (Nguyen & Phan, 2024) utilized deep learning models for concrete strength prediction, which introduced Convolutional Neural Networks (CNN) for feature self-learning, thereby improving prediction accuracy.

In addition to predictive models, researchers have explored the application of uncertainty analysis and adjustment methods in concrete strength prediction. For instance, a report (Zheng et al., 2023) that proposed a Bayesian network combined with Monte Carlo simulation for uncertainty analysis in concrete strength, which effectively quantified experimental data uncertainty and provided reasonable adjustments to enhance reliability and accuracy. Some pundits (Kaboosi et al., 2020) integrated Grey Relational Analysis with machine learning to develop a novel concrete strength evaluation model. This approach improved prediction accuracy through a robust adjustment mechanism, even in cases of incomplete or missing data. Figure 1 (Al-Mughanam et al., 2020; Nazari, 2013; Gao, 1997; Asteris et al., 2021b; Moodi et al., 2018; Ji et al., 2006) summarizes the features used in predictive models from various studies. Most existing concrete strength prediction models are based on material characteristics, such as cement, water, coarse/fine aggregates, and admixtures, with limited incorporation of curing age as a feature. However, in practical engineering, concrete strength prediction faces numerous challenges, including data diversity, complexity, and uncertainty (Alwash et al., 2016). Concrete strength data often contain noise, missing values, and measurement errors, which pose challenges to model generalization and prediction accuracy. Additionally, current machine learning methods generally rely on large amounts of training data, which impose higher requirements for data collection and processing (Yu et al., 2021).

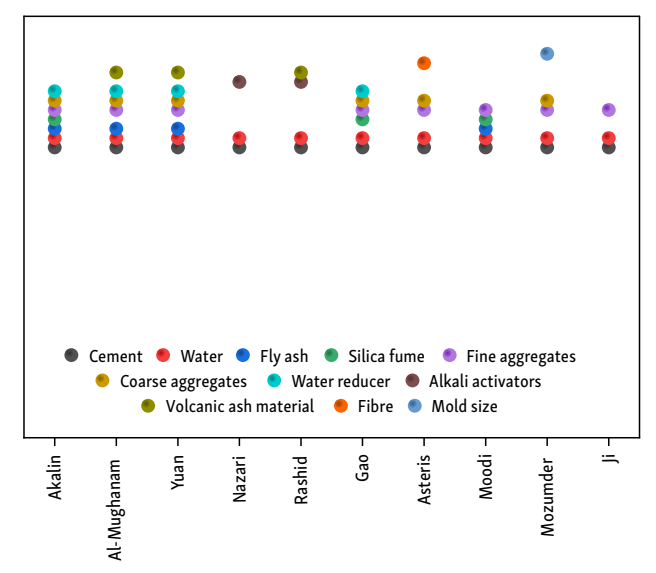


Figure 1. Features used in each model (Al-Mughanam et al., 2020; Nazari, 2013; Gao, 1997; Asteris et al., 2021b; Moodi et al., 2018; Ji et al., 2006)

Table 1. Applications of machine learning techniques in concrete studies

Author	Akalin et al. (2010)	Yuan et al. (2014)	K. Rashid and T. Rashid (2017)	Wu et al. (2024)	Mozumder et al. (2017)
1	A statistical model of second-order polynomials	Genetic algorithm	Fuzzy logic (FL)		Support vector machines (SVM)

Therefore, developing a robust and efficient concrete strength evaluation and adjustment model that integrates machine learning techniques with uncertainty analysis in highly uncertain environments has become a critical direction for current research.

In this study, 1,090 concrete compressive strength datasets were collected from actual construction projects, which covered various curing ages and strength grades. These datasets were used to establish an evaluation and adjustment model for construction quality data uncertainty. The study employed two primary modules: data fitting and data prediction, to adjust and cleanse deviations caused by environmental factors or human operations, thereby improving the reliability and rationality of construction quality data. Firstly, concrete data with a curing age of 28 days and different strength grades were selected to explore the mathematical model describing the relationship between strength and grade. Outliers and deviating points were cleansed and adjusted. Next, the influence of different curing ages on construction quality data was analyzed. Although certain rationality and patterns were observed, the data exhibited some degree of dispersion and significant fluctuations, including a few outliers. Differences in construction conditions across different locations, and the inclusion of fibers or expansive agents to enhance crack resistance in certain areas, were found to significantly promote the early strength development of concrete. Finally, a detailed analysis of construction quality data uncertainty at the same construction location was conducted. This accurately illustrated the strength development patterns across various curing ages, which ensured overall project quality and safety. This method provides a scientific basis for construction decision-making.

2. Project background and data processing methods

2.1. Project background

Sichuan Provincial Building Industry Park Project officially commenced construction on March 21, 2022, in Tianfu New Area, Sichuan. This project focuses on research and incubation surrounding urban renewal and smart building technologies. It aims to become the first demonstration project in Southwest China to integrate three building standards: Green Building Three-Star, Nearly Zero Energy Building, and Zero Carbon Building.

As a key municipal project, the total investment amounts to 309 million RMB. The site spans 45 acres, with a total floor area of approximately 63,000 square meters, including 53,000 square meters of above-ground structures and nearly 10,000 square meters underground. The floor area ratio is 1.81, and the building density reaches 40%. As shown in Figure 2, the project comprises six individual buildings. The basement includes two entrances and one exit, providing 258 parking spaces for motor vehicles. Building 1 serves as the primary office building, featuring conference halls and exhibition spaces. Building 2 is an all-prefabricated staff canteen with two private dining rooms accommodating 34 people and a general dining area for over 400 people. Building 3 is a staff dormitory with 223 rooms, housing up to 446 people, with standard rooms measuring 25.56 square meters. Building 4 houses the testing center laboratories, with a first-floor standard height of 7.2 meters (with partial areas reaching 16.2 meters), second- and third-floor heights of 4.8 meters, and a fourth-floor height of 4.0 meters.



Figure 2. Overall schematic of the project

This project focuses on urban renewal, retrofitting existing buildings, zero-carbon and low-carbon architecture, smart buildings, intelligent construction, and building safety and earthquake resistance. It aims to undertake a series of technical breakthroughs and project incubations. By integrating green, healthy, and intelligent building principles, the project achieves an overall prefabrication rate exceeding 36%, which strived to become a nationally exemplary green and smart industrial park.

2.2. Evaluation and adjustment model

The study collected a total of 1,090 concrete cube compressive strength test reports for analysis. These reports were provided by Sichuan Jianyan Shanjian Technology Development Co., Ltd., with oversight from Sichuan Construction Engineering Supervision Co., Ltd. The compressive strength tests for the concrete cube specimens were conducted in accordance with the national standard "Standard for Test Methods of Mechanical Properties of Concrete" (GB/T 50081-2019) (Ministry of Housing and Urban-Rural Development of the PRC, 2019). Although all 1090 observations used in this study were obtained from the Sichuan Construction Industrial Park project which ensure high data quality and internal consistency. However, this data set inevitably limits the external validity of the model results. To address this limitation, a detailed comparison of data from different construction locations within the project was conducted, preliminarily verifying the model's applicability across multiple construction environments. Future research will focus on expanding the data sources to encompass projects from various regions and types, thereby further validating and refining the model's generality and enhancing its reliability in broader engineering applications.

During the compressive strength testing of concrete specimens, if the difference between the maximum or minimum value and the median value exceeds 15%, the median value is adopted. If both the maximum and minimum values deviate from the median by more than 15%, the test data for that batch is considered invalid. However, due to various influencing factors such as transportation, pouring, and curing conditions, significant variations may still occur in concrete of the same strength even after the same curing duration. Moreover, differences in testing methods, worker proficiency, and instrument calibration can also impact the test results (Hariri-Ardebili et al., 2024). Consequently, using a fixed deviation between the maximum or minimum value and the median as a criterion for data validity does not fully reflect real-world construction scenarios. This approach may erroneously classify valid data as invalid or vice versa. To accurately assess the compressive strength of concrete specimens, it is essential to establish a new strength adjustment method. This method should dynamically determine the acceptable deviation range of concrete strength based on existing test data rather than relying on fixed differences between the maximum, minimum, and median values. This approach

will help identify outlier data, correct deviations, and construct a dynamic model for predicting future compressive strength at different curing ages.

Based on the provided compressive strength testing database, the data is categorized into two types: one consists of test results for specimens of different strength grades at a curing age of 28 days, and the other includes results for specimens of the same strength grade across different curing ages. To further refine the analysis of specimens of the same strength grade at varying curing ages, testing data from the same construction section was selected to evaluate the accuracy of model.

The specific steps for establishing the evaluation and adjustment model for construction quality data uncertainty are as follows.

The arithmetic mean of n measurements in Group j is defined as the reference strength and calculated by Eqn (1):

$$a_{vj} = \frac{\sum_{i=1}^{n} a_i}{n},\tag{1}$$

where a_{vj} denotes the mean of measured strength in Group j, a_i denotes the measured strength of the i-th specimen, and n is the number of specimens.

The maximum and minimum allowable error margins within the group which reflects data dispersion, are then calculated by Eqns (2) and (3):

$$v_{Mj} = \frac{\sum_{1}^{n} (a_i - a_{vj})^2}{n}; \tag{2}$$

$$v_{mj} = \frac{(a_a - a_{ab})^2 + (a_b - a_{ab})^2}{2},$$
(3)

where v_{Mj} and v_{mj} represent the maximum and minimum allowable error margins for Group j, and a_{ab} is the mean of the two most similar measurements (a_a and a_b).

This dynamic approach replaces the traditional fixed 15% threshold. For example, $v_{Mj} = 4.0$ corresponds to a fluctuation range of ± 2.0 MPa.

Using the historical variances from the first j Groups, the allowable error margins for the next group is predicted by Eqns (4) and (5):

$$V'_{Mj} = \frac{\sum_{1}^{j} v_{Mj}}{n}; \tag{4}$$

$$V'_{mj} = \frac{\sum_{j=1}^{j} v_{mj}}{n},\tag{5}$$

where V'_{Mj} and V'_{mj} are the predicted maximum and minimum allowable error margins based on the previous i Groups.

Finally, an iterative "predict-measure-feedback" loop is implemented to update the mean and variances by Eqns (6), (7), and (8):

$$A_{ij} = \frac{\sum_{i=1}^{n} a_i'}{n}; \tag{6}$$

$$V_{Mj} = \frac{\sum_{i=1}^{n} (a'_{i} - A_{vj})^{2}}{n}; \tag{7}$$

$$V_{mj} = \frac{(a'_{a} - a'_{ab})^{2} + (a'_{b} - a'_{ab})^{2}}{2},$$
(8)

where A_{vj} , V_{Mji} , V_{mj} corresponds to a_{vj} , v_{Mji} , v_{mji} , and represent the adjusted mean, maximum, and minimum allowable error margins for Group j. a_i' , a_a' , a_b' , a_{ab}' corresponds to a_i , a_{ai} , a_{ab} , a_{ab} , and represent the adjusted measurements.

2.3. Construction quality data adjustment method

As shown in Table 2: (a) When the actual strength falls within the minimum allowable error range, it is considered a valid measurement and retained. (b) When the actual strength exceeds the maximum allowable error range, it is deemed invalid and removed from the dataset. (c) If the actual measurement lies outside the minimum allowable error range but remains within the maximum allowable error range, it requires adjustment. The definitions of the different ranges are determined by Eqns (9), (10), and (11).

As shown in Eqn (12), the adjustment method employs a weighted approach, combining predicted strength with measured strength. The weight for the predicted strength is set to 1, while the weight for the measured strength is

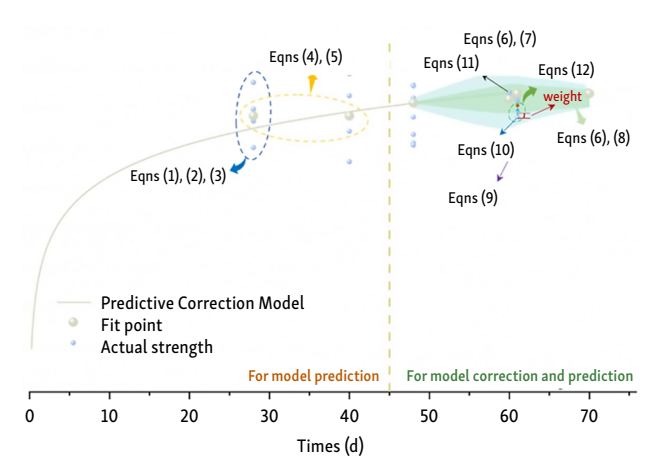


Figure 3. Distribution of computational formulas

Table 2. Evaluation methods

Graphical representation Treatment and engineering significance Falls within the green Retain original value; Original value lies within the $V_a \in \left[V_p - V_{mi}, V_p + V_{mi}\right]$ interval expected fluctuation range $V_a \in \left[V_p - V_{Mj}, V_p - V_{mj}\right] \cup \left[V_p + V_{mj}, V_p + V_{Mj}\right]$ Falls within the blue Apply weighted adjustment (Eqn (12)); Original value interval is reliable but requires adjustment $V_a \in \left[0, V_p - V_{Mj}\right] \cup \left[V_p + V_{Mj}, +\infty\right]$ Falls outside these Exclude; Original value contains significant error intervals

Notes: V_a denotes the actual measured strength and V_p denotes the model-predicted strength.

calculated based on its distance from the boundary of the minimum allowable error margins. This ensures that the date adjustment is more accurate and reliable:

$$V_{c} = \frac{V_{p} + (|V_{a} - V_{p}| - V_{mj}) \cdot V_{a}}{1 + (|V_{a} - V_{p}| - V_{mj})},$$
(12)

where V_a denotes the adjusted strength. The farther V_a lies from the minimum allowable error margins, the greater its weight in the adjustment. The adjusted strength V_c then fluctuates around V_p . For example, if $V_p = 35$ MPa, $V_a = 36.2$ MPa, $V_{mj} = 1$ and $V_{Mj} = 2$, the weight of V_a is 0.2, and the adjusted strength becomes 35.2 MPa, which falls within the minimum allowable error margins. Figure 3 illustrates which portions of the workflow correspond to each equation, thereby aiding readers in understanding the methodology.

3. Evaluation and adjustment of construction quality data at different strength grades

In engineering projects, different structural components use varying strength grades of concrete, determined by a comprehensive evaluation of structural safety, construction environment, cost-effectiveness, and functional reguirements (Igbal et al., 2024). For load-bearing components such as foundations, columns, and beams, higher strength concrete is typically chosen to ensure structural stability and long-term safety, as these components bear significant loads. In contrast, non-load-bearing components, such as infill walls and flooring, can use lowerstrength concrete, reducing construction costs. Additionally, the construction environment imposes varying durability requirements on concrete. For instance, underground environments often demand higher strength and superior anti-corrosion performance to withstand complex subterranean conditions. Functional requirements of specific components also dictate concrete strength selection, with high-load-bearing components necessitating higherstrength concrete grades.

By appropriately selecting suitable strength grades of concrete, structural safety and durability can be ensured while enhancing project cost-effectiveness and construction efficiency. This section investigates and analyzes the results of construction quality data processing for concrete of different strength grades at a curing age of 28 days.

3.1. Prediction and adjustment at different strength grades

Figure 4 illustrates the prediction and adjustment results for construction quality data of concrete at different strength grades. The first three groups of concrete data (C15, C20, C25) were selected as fitting data. Based on their development trends, the data exhibit an initial linear relationship, which was used to establish a preliminary fitting model. Through this model, the predicted strength of C30 concrete was calculated as 39.24 MPa, with a maximum permissible error of 2.47 MPa. Since this group contained several identical measurements, the minimum permissible error was set to 0.

According to the evaluation methods and adjustment formulas presented in Table 2, the actual measured values of C30 were processed. Before adjustment, the mean strength of C30 was 38.89 MPa, which increased to 39.16 MPa after adjustment. This improvement was primarily due to the adjustment method effectively removing some outlier data, which reduced the strength distribution range and made the adjustment values more accurately reflect the actual performance of the concrete.

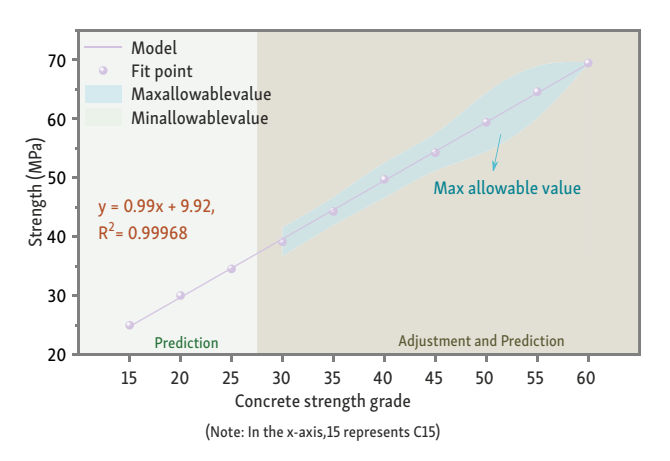
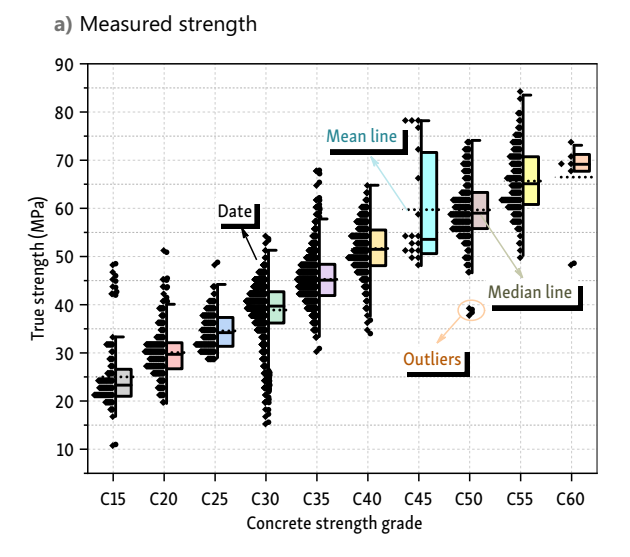


Figure 4. Prediction and adjustment model at different strength grades

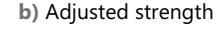


After obtaining the adjusted C30 strength, the model was updated using data from C15, C20, C25, and the adjusted C30. This updated model was then used to predict and adjust the strength of C40 concrete. The fitting and prediction process continued up to the C60 strength grade, where the coefficient of R² reached 0.99968. This result indicates that the model provides an exceptionally high level of explanatory power for the linear relationship between concrete strength and strength grade. The fitting results were nearly ideal, capable of describing this relationship with remarkable precision. This further confirms high reliability in predicting and adjusting concrete strength of this model.

Within the range of concrete strength grades from C30 to C60, the maximum permissible error showed a gradual increasing trend. This trend suggests that higher-strength concrete may exhibit greater variability or uncertainty in its performance during construction. Identifying this permissible error range facilitates a more accurate assessment of the rationality of actual strength data and helps to identify potential outliers, which can improve the precision of construction quality management.

3.2. Construction quality data evaluation at different strength grades

Figure 5 presents a comparison between the real strength data and the adjusted strength data for different strength grades. It can be observed that the real strength data for different strength grades generally follows a normal distribution, but the data exhibit considerable dispersion, i.e., the variance (σ^2) is high. After adjustment, the dispersion of the data is significantly reduced, and the distribution becomes more concentrated, with a decrease in variance (σ^2) . Taking C30 as an example, which is the first strength grade to be predicted and adjusted, the adjusted strength increased by 0.27 MPa compared to the real strength. This increase is primarily due to the higher dispersion of the data below the mean in the real strength dataset. After



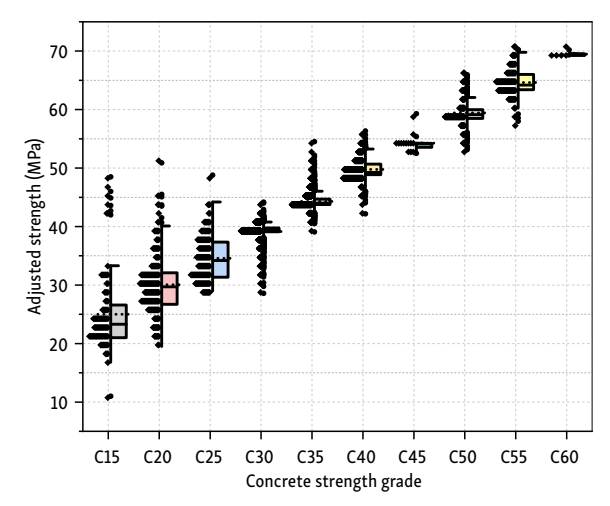


Figure 5. Strength statistics chart at different strength grades

adjustment, extreme outliers with low values were cleaned, and some data points were adjusted to align with the predicted values, which significantly reduced the overall dispersion and making the result more rational and convincing.

In the C45 data group, the mean real strength was 59.71 MPa, whereas the mean adjusted strength dropped to 54.26 MPa. This change can be attributed to two factors: first, the dataset for this group had fewer data points, and the sample distribution lacked regularity. The data points were mainly concentrated in the lower-value region, so the adjustment process brought the data closer to this region. Second, since the mean real strength of C50 was 59.66 MPa, with the adjusted mean of 59.43 MPa, if the real mean strength were used as a sole basis, the strength values of C45 and C50 would be nearly identical, which does not reflect the actual situation. Therefore, the adjusted strength values are more consistent with the realworld scenario. For the C60 group, there were clearly two outliers in the real strength data, which pulled the overall mean strength lower. After adjustment, these outliers were effectively cleaned, and the strength data returned to normal levels. Overall, the prediction and adjustment process made the strength data more reasonable, which closely aligned with actual conditions and enhanced the accuracy and consistency of the data.

3.3. Evaluation and adjustment model coefficients change at different strength grades

Figure 6 presents the trend of changes in the fitting coefficients at various strength grades. It is evident that coefficient *a* increases gradually, while coefficient *b* decreases continuously. Coefficient *a* reflects the sensitivity of strength increase to the strength grade during the fitting process, which represents the increment in strength caused by an increase in strength grade. In the fitting pro-

cess from C30 to C40, coefficient a grows most rapidly, which can indicate that the strength of concrete increases more significantly when transitioning from lower to higher strength grades. In the range from C50 to C60, coefficient a stabilizes, indicating that the performance improvement of concrete in the high-strength grade range becomes more gradual, and the linear relationship in the fitting model approaches saturation.

Coefficient *b* represents the strength value at zero strength grade (theoretically). Although this value does not have direct physical significance in practical engineering, it reflects the baseline offset of the fitting model. As the strength grade increases, coefficient *b* exhibits some fluctuations, and it reaches a local peak at C45, followed by a decrease at C55 and C60. This changing trend indicates how the fitting model adjusts at different strength grades.

The variations in coefficients a and b reflect the differences in the mechanical properties of concrete at different strength grades, which provide theoretical support for the selection of the appropriate strength grade of concrete in engineering. In the high-strength grade range, the linear characteristics of the model gradually weaken, and that is mean that more non-linear analytical methods may be needed to accurately describe the performance of high-strength concrete.

The proposed model dynamically determines upper and lower allowable error bounds based on incoming inspection data, enabling automatic cleansing and adjustment of outliers. This mechanism allows real-time adaptation to changing field conditions. In contrast, Bayesian-network approaches (Imam et al., 2021; Ragaa et al., 2025; Slonski, 2010) and grey relational analysis (Behnood & Golafshani, 2018; Gong et al., 2023; Islam et al., 2025; G. Singh & N. Singh, 2025) typically rely on preset parameters or static thresholds, limiting their ability to respond dynamically to data fluctuations.

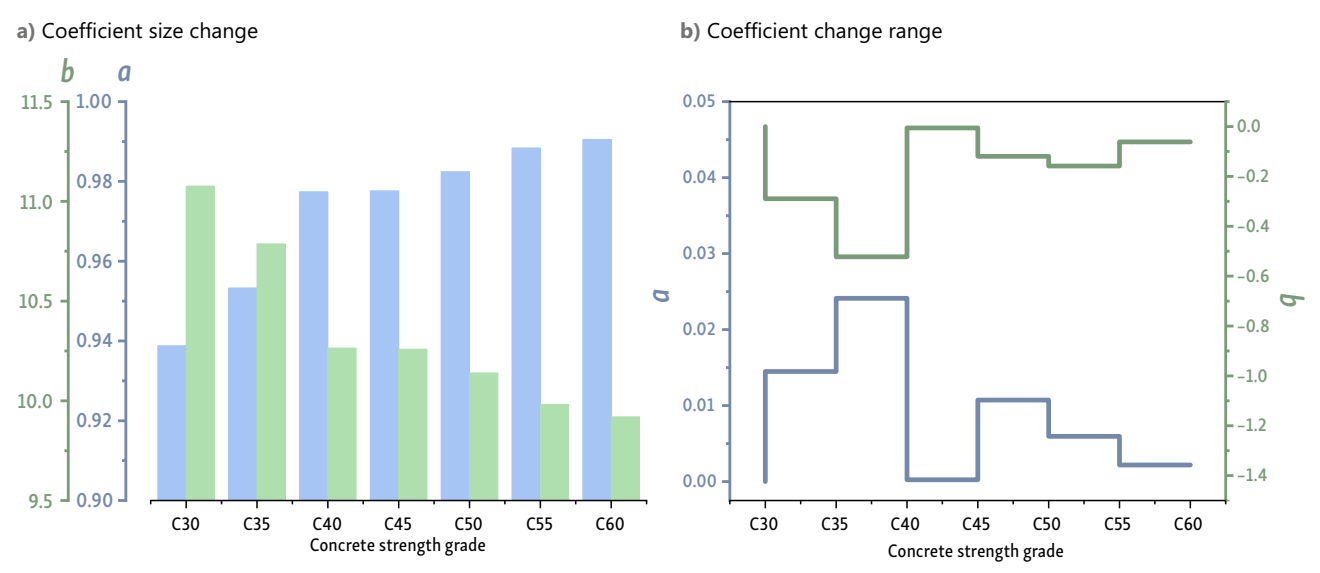


Figure 6. Variation of coefficient values during the fitting process

3.4. Multiple index consideration

To further assess predictive performance and generalization ability, three additional error metrics were employed: root mean square error (RMSE), mean absolute error (MAE), and mean absolute percentage error (MAPE). Moreover, a five-fold cross validation procedure was implemented to examine the robustness of the model.

As shown in Figure 7, a systematic analysis was conducted on concrete test data across all strength grades, and the results demonstrate that the proposed data processing method delivers differentiated optimization effects. In the medium to high strength range (C30 through C60), the improvements are most pronounced. For C60, the standard deviation was reduced by 94.4% and the MAPE dropped from 17.0% to 0.4%, illustrating exceptional noise reduction capability. In the C30 to C55 range, standard deviations decreased by between 63.8% and 85.5%, with C45 achieving the greatest reduction of 85.5%. Error metrics also improved markedly: the MAPE for C30 declined from 12.6% to 2.3%, and for C35 from 8.9% to 2.2%. Notably, the RMSE for C60 fell from 8.74 MPa to 0.35 MPa, highlighting the method's special efficacy for high strength concrete.

From an engineering perspective, these findings indicate that the method significantly enhances the reliability and consistency of strength measurements for medium and high strength concretes, with especially pronounced

gains for C45 and C60. Overall, this approach provides important technical support for concrete strength testing, particularly in quality control applications involving medium to high strength materials.

4. Evaluation and adjustment of construction quality data at different curing ages

4.1. Prediction and adjustment at different curing ages

During the curing process of concrete, the compressive strength typically increases as the hydration of the binder materials progresses. Figure 8 shows the strength prediction and adjustment results of concrete with different strength grades at various curing ages. Due to the limited data for C15, C20, C25, C45, and C60 (with fewer than three data points for each curing age), these strength grades are not included in the detailed analysis.

In the analysis of the C30 data set, a noticeable discrepancy between the fitting points and the prediction model was observed, particularly for the second fitting point. The strength at this point was even higher than that at later curing ages. Specifically, at 21 days of curing, the strength reached 39.93 MPa, which surpassed the 39.52 MPa measured at 33 days. This anomaly may be attributed to the fact that the statistical sample includes all C30 concrete

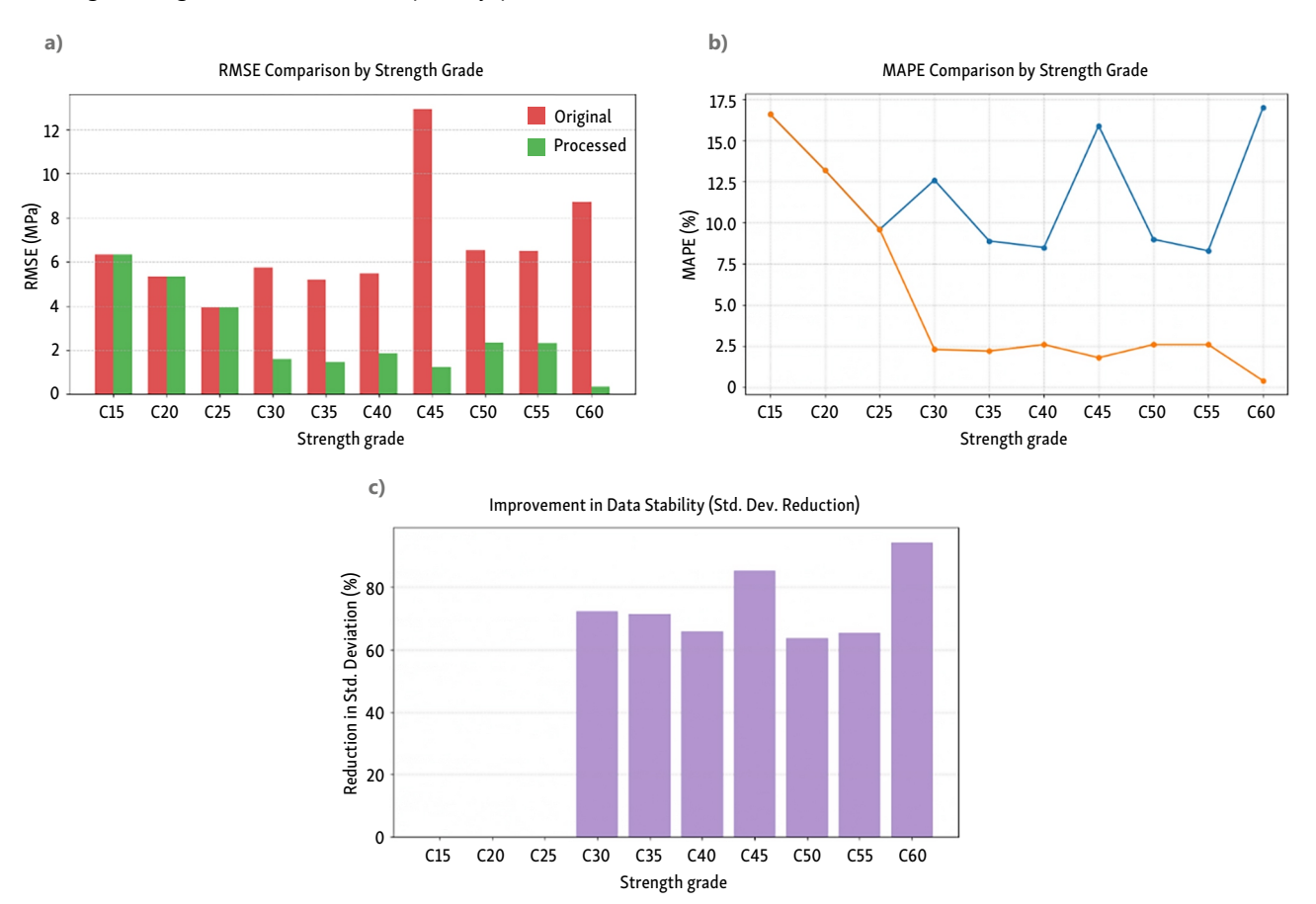


Figure 7. Prediction performance evaluation: a – RMSE of original and adjusted data; b – MAPE of the original and adjusted data; c – Percentage reduction of standard deviation

specimens, which could have different strengths due to variations in transportation time, manufacturing methods, and curing conditions. Additionally, some special locations may have incorporated crack-resistant fibers to enhance cracking performance, which also increased the strength of concrete. The model for the C30 data set, affected by anomalous data at 12 and 21 days of curing, resulted in an R² value of only 0.945304. This suggests that the relationship between curing age and strength is generally represented, but is influenced by these outliers.

The fitting results of the C35 and C40 data sets are similar. Both exhibit cases where fitting points within the fitting range are higher than the prediction model, while some fitting points in the prediction range fall below the

model. This phenomenon may be due to the inclusion of micro-expansion fibers in some specimens during early curing ages, which can result in rapid strength growth that stabilizes in a short period. At the same time, the statistical samples also include specimens without fiber reinforcement, leading to a trend that fitting points slightly exceed the prediction model. This deviation causes the model to predict continued strength growth in the middle and late curing stages, whereas, in reality, the strength plateaus. Nonetheless, the R² values of the models for the C35 and C40 data sets reach 0.98861 and 0.98875, respectively, which can indicate a good fit between the adjusted strength values and the actual strength values.

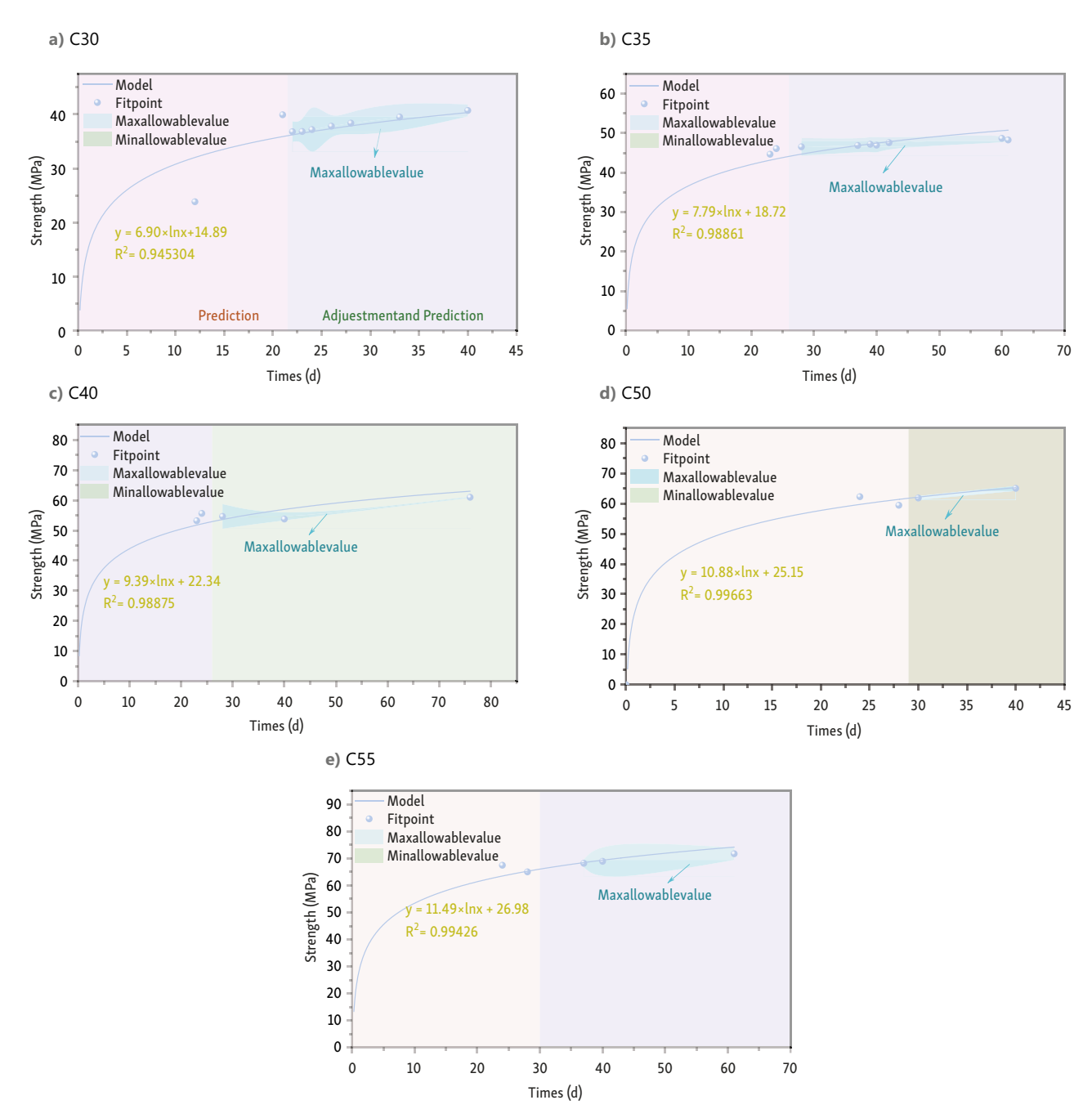


Figure 8. Prediction and adjustment model at different curing ages

For high-strength concretes C50 and C55, the prediction and adjustment models demonstrate high accuracy, with R² values of 0.99663 and 0.99426, respectively. As concrete strength typically grows rapidly during early curing ages and stabilizes in the middle and later stages, the models effectively capture this "rapid-growth to steady-state" behavior. The distribution of fitting points in Figure 8d and 8e is dense and almost entirely within the range of maximum allowable error, which indicate minimal strength data fluctuations for C50 and C55 concretes. This contributes to higher model reliability. The distribution of prediction points reveals no significant anomalies or outliers, further confirming the high quality of the data. From a material perspective, C50 and C55 concretes commonly use high-performance cement, optimally graded aggregates, and efficient admixtures, which improve the uniformity and stability of concrete strength. These material characteristics provide a solid foundation for the high fitting accuracy of the models. Additionally, the preparation of C55 concrete may involve optimized curing measures (e.g., high humidity), which help ensure strength growth aligns closely with the model predictions.

4.2. Construction quality data evaluation at different curing ages

Figure 9 illustrates the actual and adjusted compressive strengths of concrete with different strength grades at various curing ages. It can be observed that the actual strength shows a relatively scattered distribution across different curing ages, especially around the critical age of 28 days, where significant fluctuations and some outliers are present. These variations may be attributed to testing conditions, material uniformity, or construction processes. In contrast, the adjusted strengths exhibit clear advantages. After model adjustments, the date adjustment display a more concentrated distribution, a smoother overall trend, and a strong correlation with curing age, particularly beyond 28 days, where the results demonstrate excellent stability. This indicates that the adjustment model effectively eliminates random errors in the data, enhancing the reliability and representativeness of the strength data. The adjusted strength values are closer to the actual conditions, which avoided overestimation or underestimation caused by experimental variations or errors. This provides a more accurate basis for assessing construction quality and prediction concrete strength in engineering projects. However, certain limitations of the model should be noted. Since the model is derived from existing data, it may not fully account for special conditions, such as extreme environments or anomalies in raw materials, which could impact strength.

Consequently, the model may exhibit deviations under extreme circumstances or in unique environments. Additionally, the model with heavy reliance on historical data could introduce systematic errors if the data samples are insufficient or contain numerous outliers. Despite these challenges, the model significantly improves the quality

of concrete strength data. To ensure comprehensive and accurate predictions, the model should be dynamically adjusted and validated using real-world experimental results. This approach can further enhance adaptability and reliability of the model, ensuring it meets the practical needs of diverse construction scenarios.

4.3. Evaluation and adjustment model coefficients change at different curing ages

Figure 10 illustrates the variations in this model coefficients across different strength grades. Coefficient *a* directly influences the strength growth rate of concrete specimens at different curing ages. As shown in Figure 10, the value of *a* increases with the strength grade of the concrete. This indicates that, in the early curing stages of high-strength concrete, strength increases more rapidly with age, which aligned with the typical trends observed in concrete strength development. Coefficient *b*, on the other hand, is a constant that represents the theoretical initial strength or baseline strength of concrete at a curing age of 1 day. As the strength grade increases, the accelerated hydration rate of concrete leads to higher early-age strength values, which is consistent with the trends depicted in the figure.

Coefficient *a* reflects material properties and is closely related to the early strength development of concrete. Factors such as the hydration rate of cement and curing conditions significantly influence early strength growth. Coefficient *b*, however, represents the initial state of the material and is considered indicative of the impact of initial conditions on strength, such as the starting level of early strength or the inherent baseline properties of the concrete, which are tied to its strength grade.

From a mathematical perspective, coefficient a captures the sensitivity of strength changes to age progression, while b represents the initial strength level. This model effectively characterizes the typical strength development behavior of concrete. Its form is well-suited to reflecting the inherent trends in concrete strength growth over time, which makes it a valuable tool for both uncertainty evaluation and the adjustment of the model.

4.4. Multiple index consideration

As shown in Figure 11, a comprehensive analysis was performed on strength test data for C30–C55 concretes at multiple curing ages to elucidate the age dependent optimization behavior of the proposed data processing method. The results indicate significant variation in optimization efficacy both among different strength grades and within the same grade across curing ages. For C30 concrete, the reduction in standard deviation ranged from 54.7% to 66.1%, with the maximum reduction of 66.1% observed at 23 days. Early age reductions in MAPE were particularly notable, decreasing from 6.3%–11.9% to 2.1%–4.6%, which demonstrates the method's capability to accurately predict early age strength development.

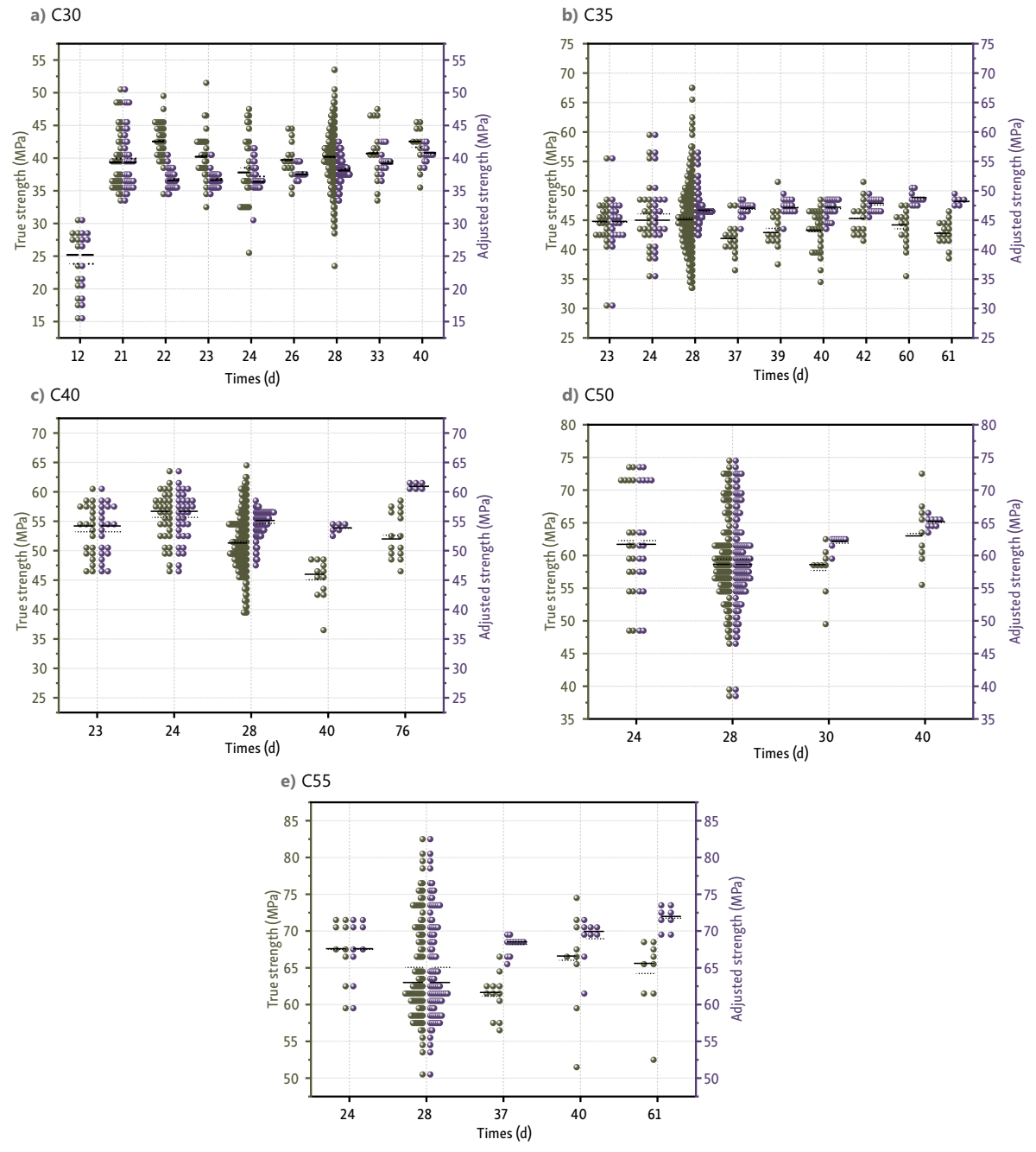


Figure 9. Statistical chart of construction quality strength at different curing ages

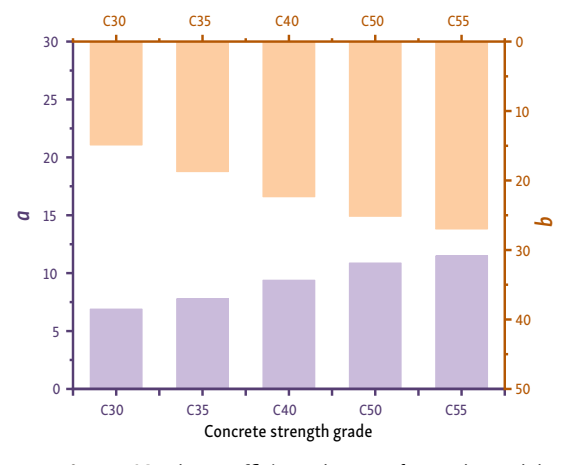


Figure 10. The coefficient changes for each model

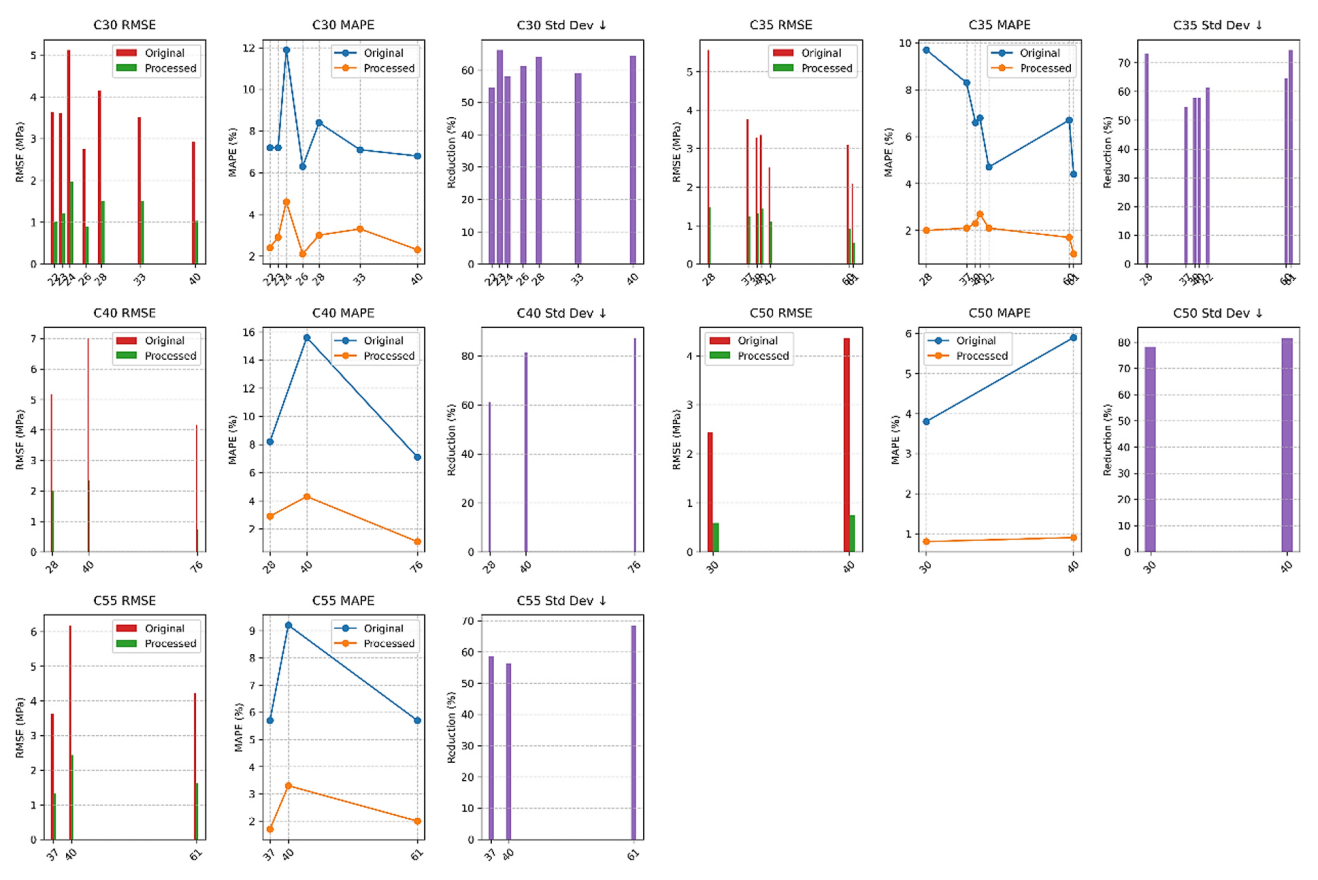


Figure 11. Model evaluation indexes at different curing ages

In the case of C35 concrete, optimization efficacy increased with curing age: the standard deviation reduction reached 74.3% at 61d, compared to 54.5% at 37d. Across all strength grades, peak optimization was achieved at approximately 40-days. At this age, standard deviations for C30, C35, C40, and C50 concretes were reduced by 64.5%, 57.8%, 81.4%, and 81.6%, respectively. This convergence corresponds to the stabilization phase of strength gain and provides critical technical support for long term structural quality assessment. Following data processing, MAPE values for all grades fell below 3%, with C50 concrete attaining the lowest MAPE of 0.8%–0.9%, thereby confirming the method's high predictive precision.

These findings confirm that the proposed data processing method effectively accommodates the strength development characteristics of concrete at different curing ages, furnishing robust data support for engineering quality control.

5. Evaluation and adjustment of construction quality data at the same construction location

As revealed in Section 4.2, concrete strength is influenced by various external factors, such as transportation time, specimen preparation methods, and curing practices. Additionally, certain special construction locations may require the incorporation of admixtures or fibers, which can further affect the strength data. To eliminate the interference of these external variables, a single construction location was selected for study. By focusing on the concrete construction quality data from this specific site, the goal is to achieve more accurate and representative predictive results.

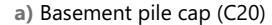
5.1. Prediction and adjustment at the same construction location

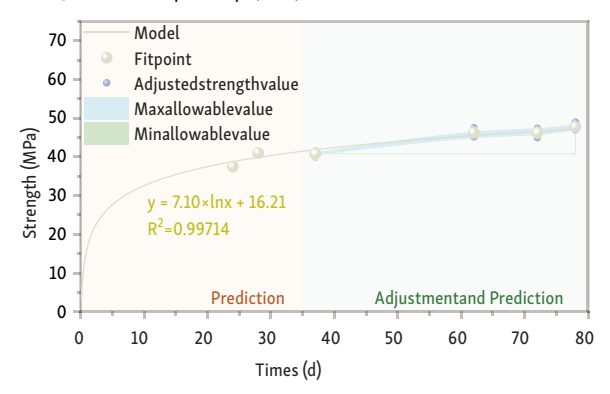
Figure 12 shows strength test data selected from the database, where multiple testing ages are available for concrete from the same construction locations. These locations represent various strength grades, including the following: basement pile cap (C20), basement stairs (C30), the surrounding basement retaining wall and top slab of the auxiliary building for Building 1 (C35), foundation slab for foundations 3, 4, and 5 (C40), basement KZL, columns, and retaining walls (C50), and basement KZL, columns, and retaining walls for Building 1, unit 2 (C55).

From the overall fitting trend in Figure 12, it is evident that the fitted of this model and data prediction are closely aligned. The coefficient of R² for all six construction locations exceeds 0.997, and the fitting points are distributed with slight fluctuations above and below the prediction curve, which indicate that the model effectively captures the strength growth patterns for concrete at various locations, and it provides a reliable predictive tool. In the early curing ages, the strength increases rapidly, and the curve's slope is steeper. As the curing age progresses,

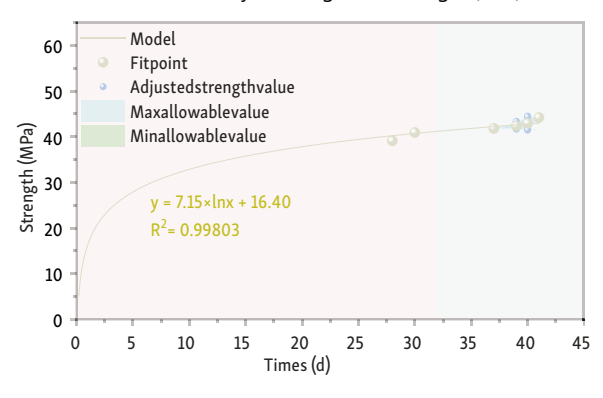
the growth rate gradually slows, and the curve flattens. This logarithmic growth trend reflects the rapid strength development during early stages of hydration, followed by a decrease in strength growth as hydration completes in the later stages. The maximum and minimum allowable error values ensure that reasonable upper and lower limits for strength are provided during prediction process of the model. These thresholds offer clear reference standards for construction quality. By establishing these standards, a reasonable strength range can be defined during construction, which helps to identify any unreasonable strength data and thus preventing potential quality issues.

In the analysis of Figure 12, it can be observed that the maximum allowable error for low-strength concrete grades (e.g., C20, C30) shows minimal and stable variation within the prediction range. This indicates that the strength behavior of low-strength concrete is more consistent across different testing ages, with lower data dispersion. Therefore, in actual construction and quality control, low-strength concrete is easier to predict and control, and its fitting accuracy is higher. As the concrete strength grade increases (e.g., C50, C55), the range and fluctuation of the maximum allowable error increase. This reflects that the actual test data for high-strength concrete is more dispersed and is influenced to a greater extent by various variables such as construction conditions, material proportions, and environmental factors. Therefore, while high-strength concrete has advantages in long-term strength performance, more attention and adjustments are required during the early stages of construction and quality control.

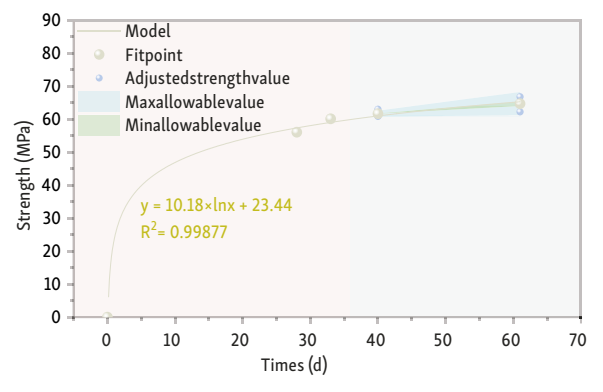




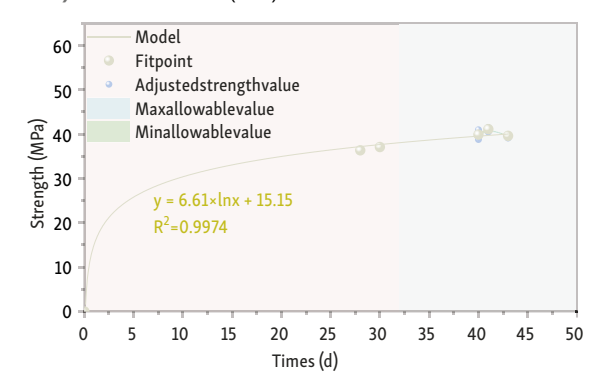
 c) The surrounding basement retaining wall and top slab of the auxiliary building for Building 1 (C35)



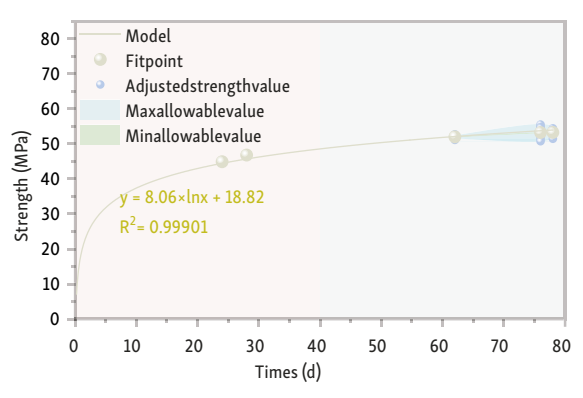
e) Basement KZL, columns, and retaining walls (C50)



b) Basement stairs (C30)



d) Foundation slab for foundations 3, 4, and 5 (C40)



f) Basement KZL, columns, and retaining walls for Building 1 (C55)

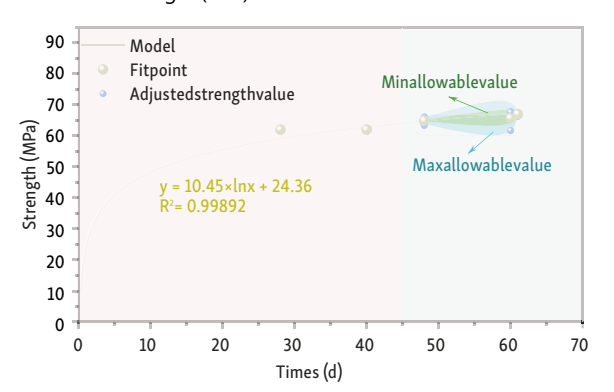


Figure 12. Prediction and adjustment of construction quality data at the same construction location

Additionally, the fitted curves in Figure 12 not only provide an effective predictive tool but also offer targeted analytical references for different construction locations. By identifying the strength development differences between low-strength and high-strength concrete at various curing ages, this can guide engineers in selecting more suitable materials during construction and implementing different quality control measures at various curing stages. For instance, in the case of low-strength concrete, early strength monitoring can be emphasized, while for highstrength concrete, particular attention should be paid to the sustained growth and stability of strength in later stages. These differentiated quality control measures for varying strength grades help improve construction quality, reduce the risk of rework, and provide a solid foundation for overall construction quality and reliability. This study also provides valuable insights for real-time comparison, hazard identification, and precise traceability of large-scale construction quality data.

5.2. Construction quality data evaluation at the same construction location

The comparison between the actual strength and adjusted strength for different construction locations is shown in Figure 13. Concrete of all strength grades demonstrates the general trend of strength increase with curing age. After the 28-day curing period, the strength of all concrete grades stabilizes. This reflects the fact that the early hydration stage after construction is a critical period for strength development. After 28 days, the rate of strength increase significantly slows down, which aligns with the basic principles of the concrete hydration reaction. High-strength concrete grades exhibit greater data fluctuations across different curing ages, likely due to the more complex mix proportions and the use of admixtures, which lead to higher dispersion in compressive strength during actual construction. Additionally, high-strength concrete relies more on good curing conditions in the early stages to ensure stable strength growth, that means small differences in construction conditions can trigger fluctuations. In contrast, the test results for low-strength concrete grades are more stable. Even across different curing ages, the data remains relatively concentrated with smaller fluctuations. This may indicate that low-strength concrete is less sensitive to mix proportions and curing conditions in actual construction. The hydration process for low-strength concrete is simpler, which results in more uniform strength development.

Within the same strength grade and curing age, the date adjustment effectively reduces the fluctuations caused by testing errors. This indicates that the adjustment process successfully adjusted the discreteness in the original data, and it made the results more consistent with the theoretical prediction curve. For each strength grade, the date adjustment displays a clearer strength growth trend, which helps to more accurately understand the strength development pattern of concrete. The adjustment pro-

cess is particularly important for high-strength concrete grades, where the original data exhibits greater discreteness. The date adjustment significantly reduces the impact of outliers, especially in the early curing ages. The adjusted strength data aligns more closely with the prediction curve that reflects a more precise strength development trend. For low-strength concrete grades, the date adjustment is very compact, with random deviations in the original test data being brought back within the prediction range. Since low-strength concrete demonstrates higher stability during the early hydration stage, the changes brought about by the adjustment are mainly subtle adjustments, which further enhances the accuracy of the prediction curve.

5.3. Evaluation and adjustment model coefficients change at the same construction location

Figure 14 shows the variation of the model coefficients for different construction locations. It can be observed that as the concrete strength grade increases, both coefficients a and b increase as well. In high-strength concrete (e.g., C50 for the basement KZL, columns, and retaining walls, and C55 for the basement KZL, columns, and retaining walls in Building 1, unit 2), these coefficients are significantly higher than those for low-strength concrete locations. This indicates that strength grade directly affects the growth characteristics of concrete at different curing ages. High-strength concrete experiences faster strength growth in the early stages, with a steeper curve in the initial phase, that means these concretes develop strength more quickly in the early curing period. In contrast, low-strength concrete (e.g., C20 for the basement pile cap and C30 for the basement stairs) shows a more gradual early strength development.

From the analysis of data from these construction locations, it can be concluded that low-strength concrete is suitable for applications where early strength is required but long-term load demands are relatively low, such as in basement stairs or foundation pile caps. Concrete in these locations can reach sufficient strength quickly after construction to support subsequent operations. High-strength concrete, on the other hand, is more suitable for critical structures with long-term load-bearing requirements, such as basement KZLs, columns, and retaining walls. Its strength growth is more stable, which provides strong durability and safety guarantees for long-term use.

5.4. Multiple index consideration

Figure 15 shows the model evaluation indexes of different construction location. For the basement frame beams, columns, and retaining walls, the standard deviation of 40-day strength data decreased by 67.1%, while the MAPE fell from 7.9% to 2.0%, representing a 74.7% reduction in error. In the basement frame beams and columns, the 48-day data exhibited an even greater reduction in standard deviation of 82.3%, with MAPE decreasing from 7.1% to 1.4%.

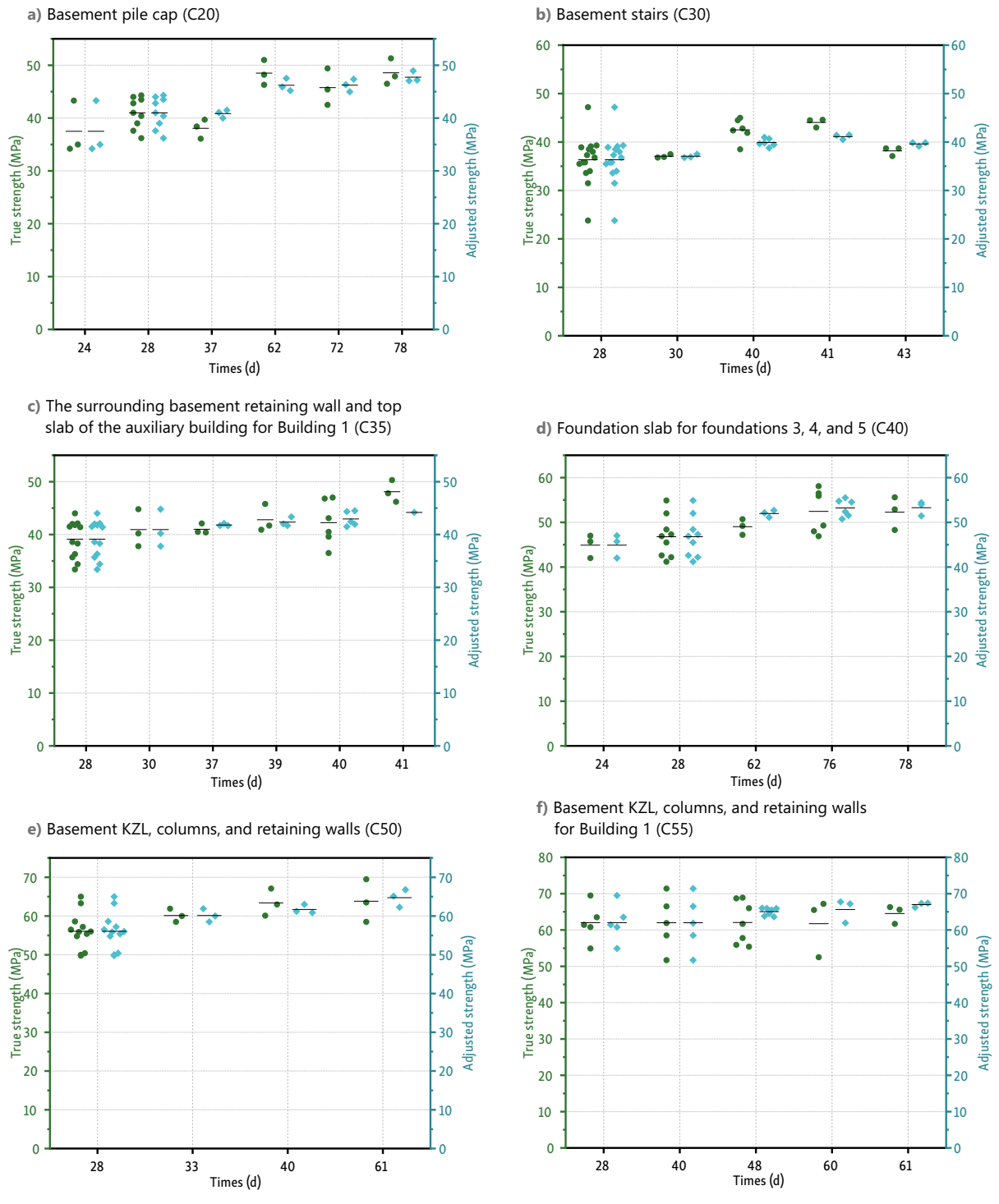


Figure 13. Statistical chart of concrete construction strength at the same construction location

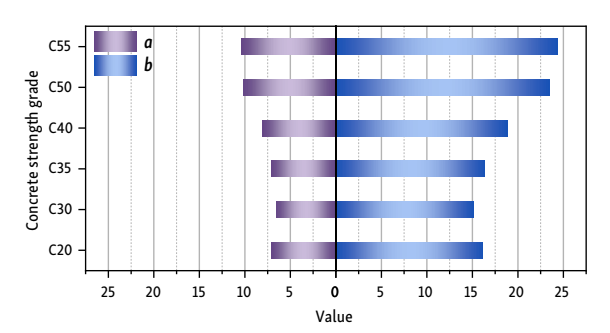


Figure 14. Coefficient changes at the same construction location

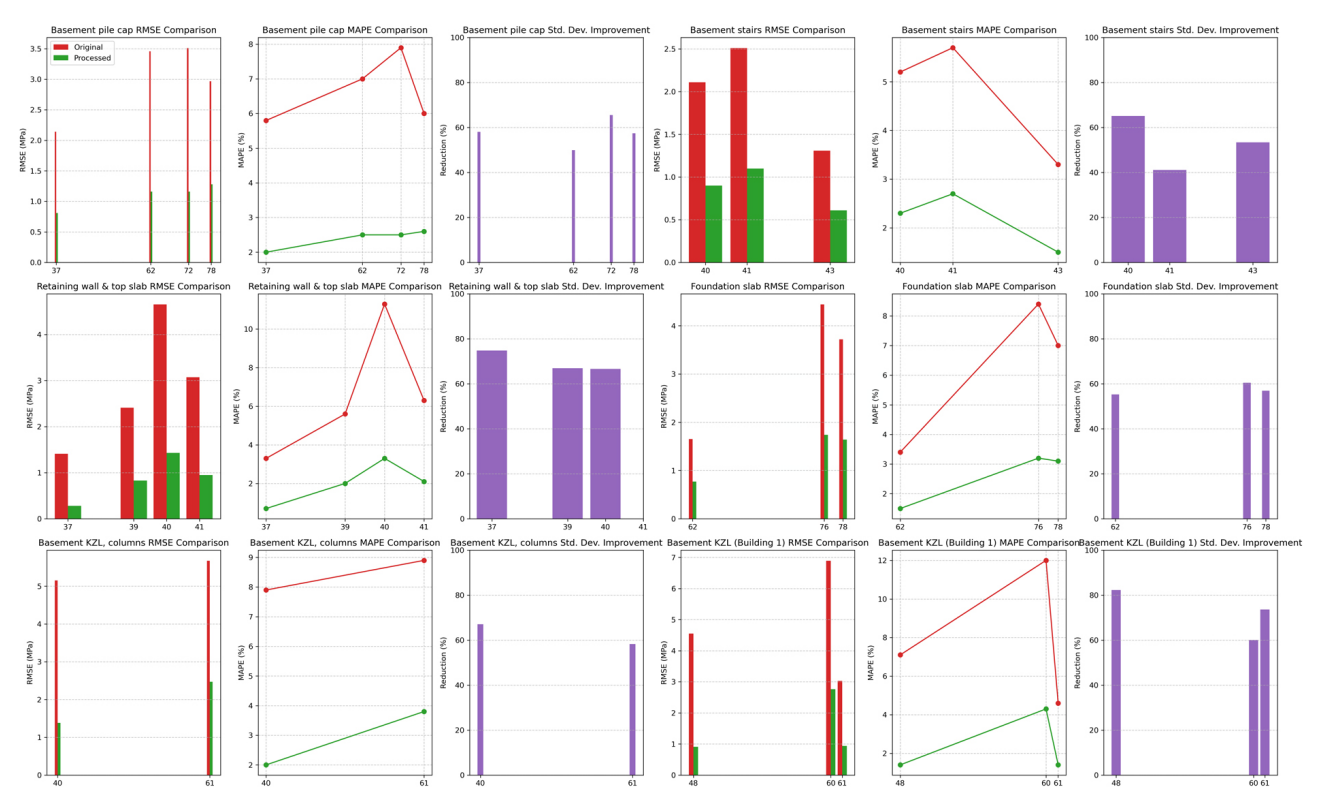


Figure 15. Model evaluation indexes at the same construction location

These findings demonstrate that the method not only effectively tightens the spread of measured values but also substantially enhances prediction accuracy. Notably, for the foundation slabs, the standard-deviation reductions for data at 62-day and 78-day remained consistently between 55.3% and 60.5%, illustrating the method's stability in processing data across extended curing periods.

From an engineering application perspective, the proposed data-processing method offers three principal advantages. First, its optimization effect is consistently strong across different structural components. Second, it performs robustly for both early-age and long-term curing data. Third, it significantly improves predictive precision, thereby reducing the risk of erroneous engineering decisions. These characteristics underscore the method's considerable value for quality control in concrete construction.

6. Conclusions

Based on the research project of the Sichuan Provincial Building Industry Park, Sichuan, this paper establishes a methodology for uncertainty evaluation and adjustment of construction quality data. This evaluation method mainly dynamically determines the deviation range of construction quality data based on existing detection data and makes adjustments based on historical data. This process helps clean up anomalous data and improves the reliability of construction quality data. Through the control of individual variables, uncertainty analysis of construction quality data for different concrete strength grades and curing ages was conducted. The results indicate that construction

quality data exhibits slight dispersion and significant fluctuations, with some outliers. Therefore, further research on the concrete construction quality data from the same construction location showed a significant improvement in the accuracy of the uncertainty evaluation and adjustment model. By analyzing these different locations in detail, engineers are able to better understand the strength development patterns of each part over time, which ensure the overall quality and safety of the project. The specific analysis of each location provides scientific basis for construction decisions, that makes project management more precise and scientific. The specific research conclusions and their engineering applications are as follows:

- Date adjustment not only reduce the fluctuation of the original data but also significantly improve the fit of the prediction model, with R² values approaching 1, indicating that the model more accurately describes the strength development pattern. The date adjustment allows the model to precisely reflect the strength development trend at different curing ages, providing more reliable prediction results for practical engineering applications.
- The date adjustment provides clear reference standards for quality control during construction. For each strength grade of concrete, the date adjustment defines reasonable strength ranges, especially by delineating the maximum and minimum permissible error values. This allows construction personnel to more effectively assess whether the actual performance of the concrete meets the expected requirements. This is crucial for improving construction efficiency and ensuring the quality of the project.

The adjustment process effectively identifies and adjusts anomalous data, which prevents overall misjudgments caused by individual test biases. This not only enhances the accuracy of data analysis but also reduces potential risks in construction decisions, providing a basis for real-time comparison of construction quality big data, hazard identification, and precise traceability.

7. Deficiency and prospect

On the basis of the primary findings, the applicability of the proposed concrete-strength adjustment and prediction model in varied engineering contexts was further investigated. The results demonstrate that, in standardized construction projects with ample data and stable conditions, the model excels at cleansing outliers and narrowing data fluctuations, thereby significantly improving predictive accuracy. However, under extreme construction conditions (such as abnormal temperature and humidity, drastic changes in construction procedures, or the use of special materials) the model may not fully capture all influencing factors, potentially leading to prediction bias. In such cases, it is recommended to integrate real-time field monitoring data and a secondary calibration mechanism to achieve higher predictive precision and practical utility.

Future research will concentrate on model optimization, cross-material applicability, and field validation. Specifically, the data preprocessing and outlier detection mechanisms will be further refined, with the incorporation of additional influencing factors such as environmental parameters and detailed construction techniques, to enhance model accuracy under specific conditions. The generalizability of the model to other construction materials will be examined to assess its potential in predicting mechanical properties and facilitating quality control across diverse material types. Furthermore, integration with real-time monitoring systems will enable dynamic calibration and feedback, ensuring sustained predictive accuracy in variable construction environments and providing timely, reliable data support for engineering decision-making.

Funding

The authors would like to acknowledge the support from the Ministry of Science and Technology of China under grant No. 2023YFC3804300 and National Science Foundation of China under grant No. 52178114.

Author contributions

Changhao Fu: Formal analysis, Writing-original draft, Writing – review & editing. Weijie Xu: Formal analysis, Funding acquisition, Project administration, Writing-original draft, Writing – review & editing. Junchi Liu: Writing – original draft, Formal analysis. Tong Guo: Formal analysis, Writing – review & editing. Qingzi Ge: Formal analysis, Writing – review & editing.

ing – original draft. Hang Bai: Formal analysis, Writing – original draft, Project administration. Tao Wang: Formal analysis, Writing – original draft.

Conflict of interest

The authors declare that they have no known competing financial interests or personal relationships that could have appeared to influence the work reported in this paper.

References

- Akalin, O., Akay, K. U., & Sennaroglu, B. (2010). Self-consolidating high-strength concrete optimization by mixture design method. *ACI Materials Journal*, *107*(4), 357–364. https://doi.org/10.14359/51663861
- Al-Mughanam, T., Aldhyani, T. H., & Alsubari, B. (2020). Modeling of compressive strength of sustainable self-compacting concrete incorporating treated palm oil fuel ash using artificial neural network. *Sustainability*, *12*(22), Article 9322. https://doi.org/10.3390/su12229322
- Alwash, M., Sbartaï, Z. M., & Breysse, D. (2016). Non-destructive assessment of both mean strength and variability of concrete: A new bi-objective approach. *Construction and Building Materials*, 113, 880–889.
 - https://doi.org/10.1016/j.conbuildmat.2016.03.120
- Arora, A., Almujaddidi, A. & Kianmofrad, F. (2019). Material design of economical ultra-high performance concrete (UHPC) and evaluation of their properties. *Cement and Concrete Composites*, 104, Article 103346.
 - https://doi.org/10.1016/j.cemconcomp.2019.103346
- Asteris, P. G., Lourenço, P. B., & Hajihassani, M. (2021a). Soft computing-based models for the prediction of masonry compressive strength. *Engineering Structures*, *248*, Article 113276. https://doi.org/10.1016/j.engstruct.2021.113276
- Asteris, P. G., Skentou, A. D., & Bardhan, A. (2021b). Soft computing techniques for the prediction of concrete compressive strength using non-destructive tests. *Construction and Building Materials*, 303, Article 124450.
 - https://doi.org/10.1016/j.conbuildmat.2021.124450
- Behnood, A., & Golafshani, E. M. (2018). Predicting the compressive strength of silica fume concrete using hybrid artificial neural network with multi-objective grey wolves. *Journal of Cleaner Production*, 202, 54–64.
 - https://doi.org/10.1016/j.jclepro.2018.08.065

https://doi.org/10.1016/S0958-9465(00)00071-8

- Bharatkumar, B., Narayanan, R., & Raghuprasad, B. (2001). Mix proportioning of high performance concrete. *Cement and Concrete Composites*, *23*(1), 71–80.
- Cao, Y., Li, P., & Brouwers, H. (2019). Enhancing flexural performance of ultra-high performance concrete by an optimized layered-structure concept. *Composites Part B: Engineering, 171,* 154–165. https://doi.org/10.1016/j.compositesb.2019.04.021
- Chen, X. Q., Zheng, D. J., Liu, Y. T., Wu, X., Jiang, H. F., & Qiu, J. C. (2023). Multiaxial strength criterion model of concrete based on random forest. *Mathematics*, 11(1), Article 244. https://doi.org/10.3390/math11010244
- Erdal, H., Erdal, M., & Simsek, O. (2018). Prediction of concrete compressive strength using non-destructive test results. *Computers and Concrete*, *21*(4), 407–417. https://doi.org/10.12989/cac.2018.21.4.407

- Feng, D.-C., & Li, J. (2016). Stochastic nonlinear behavior of reinforced concrete frames. II: Numerical simulation. *Journal of Structural Engineering*, 142(3), Article 04015163. https://doi.org/10.1061/(ASCE)ST.1943-541X.0001443
- Feng, D., Ren, X., & Li, J. (2016). Stochastic damage hysteretic model for concrete based on micromechanical approach. *International Journal of Non-Linear Mechanics*, 83, 15–25. https://doi.org/10.1016/j.ijnonlinmec.2016.03.012
- Gao, F.-L. (1997). A new way of predicting cement strength Fuzzy logic. Cement and Concrete Research, 27(6), 883–888. https://doi.org/10.1016/S0008-8846(97)00081-1
- Gong, S., Bai, L., Tan, Z., Xu, L., Bai, X., & Huang, Z. (2023). Mechanical properties of polypropylene fiber recycled brick aggregate concrete and its influencing factors by gray correlation analysis. *Sustainability*, 15(14), Article 11135. https://doi.org/10.3390/su151411135
- Graybeal, B. A. (2007). Compressive behavior of ultra-high-performance fiber-reinforced concrete. ACI Materials Journal, 104(2), 146–152. https://doi.org/10.14359/18577
- Hariri-Ardebili, M. A., Mahdavi, P., & Pourkamali-Anaraki, F. (2024). Benchmarking AutoML solutions for concrete strength prediction: Reliability, uncertainty, and dilemma. Construction and Building Materials, 423, Article 135782. https://doi.org/10.1016/j.conbuildmat.2024.135782
- Iqbal, A. M., Irfan-ul-Hassan, M., Siddiqui, J. A., & Javed, N. (2024). Exploring engineering properties of sustainable multi-grade concrete: Materials, structural, and environmental aspects. Structural Concrete, 25(5), 3966–3992. https://doi.org/10.1002/SUCO.202300971
- Imam, A., Salami, B. A., & Oyehan, T. A. (2021). Predicting the compressive strength of a quaternary blend concrete using Bayesian regularized neural network. *Journal of Structural Integrity and Maintenance*, 6(4), 237–246. https://doi.org/10.1080/24705314.2021.1892572
- Islam, S. R., Mutsuddy, R., & Shahid, N. B. (2025). Gray correlation coefficient analysis on the mechanical properties of nylon fiber reinforced recycled aggregate concrete with GGBS. *Civil Engineering Journal*, 11(3), 932–949. https://doi.org/10.28991/CEJ-2025-011-03-07
- Ji, T., Lin, T., & Lin, X. (2006). A concrete mix proportion design algorithm based on artificial neural networks. *Cement and Concrete Research*, 36(7), 1399–1408. https://doi.org/10.1016/j.cemconres.2006.01.009
- Kaboosi, K., Kaboosi, F., & Fadavi, M. (2020). Investigation of greywater and zeolite usage in different cement contents on concrete compressive strength and their interactions. *Ain Shams Engineering Journal*, 11(1), 201–211. https://doi.org/10.1016/j.asej.2019.08.008
- Li, H., Chung, H., & Li, Z. (2024). Compressive strength prediction of fly ash-based concrete using single and hybrid machine learning models. *Buildings*, 14(10), Article 3299. https://doi.org/10.3390/buildings14103299
- Lorenzi, A., Silva, B., & Barbosa, M. (2017). Artificial neural networks application to predict bond steel-concrete in pull-out tests. *Revista IBRACON de Estruturas e Materiais*, 10(5), 1051–1074. https://doi.org/10.1590/s1983-41952017000500007
- Ministry of Housing and Urban-Rural Development of the PRC. (2019). Standard for test methods of concrete physical and mechanical properties (GB/T 50081-2019).
- Moodi, Y., Mousavi, S. R., & Ghavidel, A. (2018). Using response surface methodology and providing a modified model using whale algorithm for estimating the compressive strength of columns confined with FRP sheets. *Construction and Building Materials*, 183, 163–170.
 - https://doi.org/10.1016/j.conbuildmat.2018.06.081

- Mozumder, R. A., Roy, B., & Laskar, A. I. (2017). Support vector regression approach to predict the strength of FRP confined concrete. *Arabian Journal for Science and Engineering*, 42(3), 1129–1146. https://doi.org/10.1007/s13369-016-2340-y
- Najafabadi, M. M., Villanustre, F., & Khoshgoftaar, T. M. (2015). Deep learning applications and challenges in big data analytics. *Journal of Big Data*, 2, Article 1. https://doi.org/10.1186/s40537-014-0007-7
- Nazari, A. (2013). Compressive strength of geopolymers produced by ordinary Portland cement: Application of genetic programming for design. *Materials & Design*, 43, 356–366. https://doi.org/10.1016/j.matdes.2012.07.012
- Nguyen, D.-L., & Phan, T.-D. (2024). Predicting the compressive strength of ultra-high-performance concrete: An ensemble machine learning approach and actual application. *Asian Journal of Civil Engineering*, 25, 3363–3377. https://doi.org/10.1007/s42107-023-00984-9
- Poorarbabi, A., Ghasemi, M., & Azhdary Moghaddam, M. (2020). Concrete compressive strength prediction using neural networks based on non-destructive tests and a self-calibrated response surface methodology. *Journal of Nondestructive Evaluation*, 39(4), Article 78. https://doi.org/10.1007/s10921-020-00718-w
- Ragaa, A. B., Al-Neshawy, F., & Noureldin, M. (2025). Al-based framework for concrete durability assessment using generative adversarial networks and Bayesian neural networks. *Construction and Building Materials*, 471, Article 140722. https://doi.org/10.1016/j.conbuildmat.2025.140722
- Rashid, K., & Rashid, T. (2017). Fuzzy logic model for the prediction of concrete compressive strength by incorporating green foundry sand. *Computers and Concrete*, *19*(6), 617–623. https://doi.org/10.12989/cac.2017.19.6.617
- Ren, L., Fang, Z., & Wang, K. (2019). Design and behavior of superlong span cable-stayed bridge with CFRP cables and UHPC members. *Composites Part B: Engineering, 164,* 72–81. https://doi.org/10.1016/j.compositesb.2018.11.060
- Singh, G., & Singh, N. (2025). Destructive and non-destructive strength performance of iron slag recycled aggregate concrete using regression and grey correlation analysis. *Measurement*, 239, Article 115422.
 - https://doi.org/10.1016/j.measurement.2024.115422
- Slonski, M. (2010). A comparison of model selection methods for compressive strength prediction of high-performance concrete using neural networks. *Computers and Structures*, 88(21–22), 1248–1253. https://doi.org/10.1016/j.compstruc.2010.07.003
- Soilan, M., Gonzalez-Aguilera, D., Del-Campo-Sanchez, A., Hernandez-Lopez, D., & Del Pozo, S. (2022). Road marking degradation analysis using 3D point cloud data acquired with a lowcost Mobile Mapping System. *Automation in Construction*, 141, Article 104446. https://doi.org/10.1016/j.autcon.2022.104446
- Wang, X. H., Fang, Z. C., & Zheng, L. (2024a). Effect of dose and types of the water reducing admixtures and superplasticizers on concrete strength and durability behaviour: A review. *Journal of Civil Engineering and Management*, 30(1), 33–48. https://doi.org/10.3846/jcem.2024.20145
- Wang, Y., Wang, X., & Li, F. (2024b). Numerical simulations study of concrete mix proportion based on fluidity. *Construction and Building Materials*, 455, Article 139236. https://doi.org/10.1016/j.conbuildmat.2024.139236
- Wu, Y., Pieralisi, R., & Sandoval, F. G. B. (2024). Optimizing pervious concrete with machine learning: Predicting permeability and compressive strength using artificial neural networks. Construction and Building Materials, 443, Article 137619. https://doi.org/10.1016/j.conbuildmat.2024.137619

- Yang, K.-H., Cho, A.-R., & Song, J.-K. (2012). Effect of water-binder ratio on the mechanical properties of calcium hydroxide-based alkali-activated slag concrete. Construction and Building Materials, 29, 504–511.
 - https://doi.org/10.1016/j.conbuildmat.2011.10.062
- Yu, Z., Shi, X., & Miao, X. (2021). Intelligent modeling of blast-induced rock movement prediction using dimensional analysis and optimized artificial neural network technique. *International Journal of Rock Mechanics Mining Sciences*, 143, Article 104794. https://doi.org/10.1016/j.ijrmms.2021.104794
- Yuan, Z., Wang, L.-N., & Ji, X. (2014). Prediction of concrete compressive strength: Research on hybrid models genetic based algorithms and ANFIS. *Advances in Engineering Software*, 67, 156–163. https://doi.org/10.1016/j.advengsoft.2013.09.004
- Yudhistira, A. T., Satyarno, I., Nugroho, A. S. B., & Handayani, T. N. (2024). Effect of construction delays and the preventive role of concrete works optimization: Systematic literature review. *TEM Journal*, *13*(2), 1203–1217. https://doi.org/10.18421/TEM132-34
- Zain, M. F. M., & Abd, S. M. (2009). Multiple regression model for compressive strength prediction of high performance concrete. *Journal of Applied Sciences*, 9(1), 155–160. https://doi.org/10.3923/jas.2009.155.160
- Zheng, J., Yao, T., & Yue, J. (2023). Compressive strength prediction of BFRC based on a novel hybrid machine learning model. *Buildings*, *13*(8), Article 1934. https://doi.org/10.3390/buildings13081934
- Zhou, W., & Zhang, X. X. (2011). Dynamic compressive response and failure behaviour of CFRP composites at high strain rates. *Advanced Materials Research*, *152*, 988–991. https://doi.org/10.4028/www.scientific.net/AMR.152-153.988